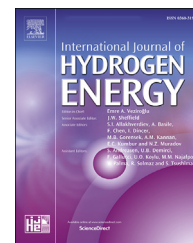




ELSEVIER

Available online at [www.sciencedirect.com](http://www.sciencedirect.com)

ScienceDirect

journal homepage: [www.elsevier.com/locate/he](http://www.elsevier.com/locate/he)

## Energetic modeling, simulation and experimental of hydrogen desorption in a hydride tank

D. Chabane <sup>a,b,\*</sup>, F. Harel <sup>b,c</sup>, A. Djerdir <sup>a,b</sup>, D. Candusso <sup>b,d</sup>, O. Elkedim <sup>a,b</sup>, N. Fenineche <sup>b,e</sup>

<sup>a</sup> FEMTO-ST, CNRS, Univ. Bourgogne Franche-Comte, UTBM, France

<sup>b</sup> FCLAB, CNRS, Univ. Bourgogne Franche-Comte Rue Thierry Mieg, F-90010 Belfort Cedex, France

<sup>c</sup> IFSTTAR AME LTE, 25 Avenue François Mitterrand, Case 24, Cit des Mobilits, F-69675 Bron cedex, France

<sup>d</sup> IFSTTAR COSYS SATIE (UMR CNRS 8029), 25 Alle des Marronniers, 78000 Versailles Satory, France

<sup>e</sup> ICB-PMDM-LERMPS, UTBM, 90010 Belfort Cedex, France

### ARTICLE INFO

#### Article history:

Received 6 September 2018

Received in revised form

30 October 2018

Accepted 1 November 2018

Available online xxx

#### Keywords:

Hydrogen

Metal hydride tank

Heat transfer

Experimental

### ABSTRACT

This paper presents a zero-dimensional (0D) model of hydride tank. The model aims to study the dynamic heat and mass transfers during desorption process in order to investigate the thermal-fluidic behaviors of this hydride tank. This proposed model has been validated experimentally thanks to a tailor-made developed test bench. This test bench allows the hydride characterization at tank scale and also the energetic characterization. The simulation results of the heat exchanges and mass transfer in and between the coupled reaction bed, show good agreement with the experimental ones. It is shown that the heat produced by a Proton Exchange Membrane Fuel Cell (PEMFC) (estimated starting from an electrical model) is enough to heat the metal alloy (FeTi) and therefore release the hydrogen with a sufficient mass flow rate to supply the PEMFC. Furthermore, the obtained results highlight the importance of the developed model for energy management of the coupling of fuel cell and hydride tank system.

© 2018 Hydrogen Energy Publications LLC. Published by Elsevier Ltd. All rights reserved.

### Introduction

Fossil fuel reserves depletion and the adverse effects of climate change have attracted global attention and pose serious threats to mankind. The development of new energy technologies based on new materials is vital if the world is to arrest the adverse effects of climate change and secure the global energy security based on sustainable and renewable energy sources. Among the various possible solutions, hydrogen appears as a very attractive energy carrier to progressively establish itself in the economy that is today based

on fossil fuels. Hydrogen has a very high energy content of 243 [kJ/mol], which makes it a very attractive, lightweight energy carrier. Aside from being the most abundant element in the universe, hydrogen is lightweight, and can be produced from all primary resources such as fossil fuels, natural gas and coal, as well as renewable resources, such as biomass and water with input from renewable energy sources (solar, wind, wave or hydro-power ...). Because hydrogen is not available anywhere as a separate element, it needs to be separated from the above mentioned sources, for which energy is necessary to do this disassociation. A variety of process technologies can

\* Corresponding author. FEMTO-ST, CNRS, Univ. Bourgogne Franche-Comte, UTBM, France.

E-mail address: [djafar.chabane@utbm.fr](mailto:djafar.chabane@utbm.fr) (D. Chabane).

<https://doi.org/10.1016/j.ijhydene.2018.11.024>

0360-3199/© 2018 Hydrogen Energy Publications LLC. Published by Elsevier Ltd. All rights reserved.

be used, they are classified in five main categories: thermochemical, electrolytic, photolytic, biological and chemical.

The experience accumulated from over a decade through different research, development and demonstration projects confirm that both fuel cell and hydrogen ( $H_2$ ) technology has a significant role to play a significant role in the green energy systems regarding the reducing addiction on fossil fuel, inhibiting pollutant and greenhouse gas emissions. A future hydrogen based society in which hydrogen will be one of the primary energy vectors will soon become a reality. The major components in the expected Hydrogen Economy involve production, storage and final use of hydrogen, e.g. in fuel cells, all of these facing considerable technological challenges. However, for the societal acceptance of these new technologies, several technical difficulties must be overcome. Therefore, it is necessary to develop news hydrogen storage devices with a high capacity, fast kinetics, long cycle life, favorable thermodynamics, controllable reversibility, cheap and high safety. There are currently three main technologies for storing hydrogen: compressed gas, liquefied cryogenic fluid, and solid in a metal hydride [1,2]. For automotive applications, using the liquid hydrogen technology as an embedded storage leads to major problems mostly due to the high energy cost of the hydrogen liquefaction process, which today can lead to 50% of the initial cost of the  $H_2$  production [3–5]. The major drawbacks related to hydrogen gas storage under high pressure [300 – 750 bar] are security and societal acceptance. Otherwise, the metal hydride storage offers the possibility to operate at very low pressure [1 – 10 bar] with a very good energy efficiency and it provides a safe way to handle hydrogen. Therefore, an important number of studies has been carried out to develop this technology in the last years [6–11]. For any hydrogen storage application, the optimum system design will vary based on operational environment, acceptable cost, and the safety and performance demands.

The information about these hydrides is generally inferred from Pressure Composition Temperature (PCT) isotherms that describe the dependence of the hydrogen equilibrium pressure to the amount of hydrogen introduced in/or extracted from the hydride at fixed temperatures. The thermodynamic parameters of the hydride-dehydride process can be obtained from the PCT. There are several methods of determining PCT properties ranging from thermogravimetric to volumetric measurements obtained by using classical Sieverts-type apparatus, chromatographic, dielectric and the method proposed in the previous work [12].

### Review of modeling approaches related to hydride tank

The absorption and desorption process in porous media of hydrides materials are considered by various mathematical models [13–18] developed in particular to meet control and design needs. The state of the art shows that the hydride bed has been studied by different research teams. From the early 1980s, a number of mathematical models including one-dimensional hydride tank [19–21] were presented to describe the thermal behavior and the mass transfer under both absorption and desorption process for various geometries of the tank.

Muthukumar P. et al. [18] presented a parametric study of a hydrogen storage device in an annular cylindrical tank device filled within  $MmNi_{4.6}Al_{0.4}$  alloy. They studied effects of various bed parameters on the storage performance such as hydride bed thickness and overall heat transfer coefficients. They observed that the average temperature of the hydriding bed and hydrogen storage capacity at different supply pressures showed good agreement with the collected experimental data.

Most of the models presented in the literature are based on 2D modeling (symmetrical with respect to the tank axis). The first two-dimensional numerical studies of a hydrogen reactor were performed by U.Mayer et al. [21]. The calculated transient behavior of reaction beds (pressure, temperature, and concentration) shows very good agreement with experimental data. The same approach has been used by A. Jemni et al. [22]. The results showed the effect of the geometry, of the inlet pressure and were used for the choice of the cooling temperature on the thermal behavior of the metal hydride. A mathematical model for a solid hydrogen storage was modeling by Y.Kaplan et al. [23]. In conclusion of their work, they found that the increase in temperature leads to the decreases of the hydrogen rate. Therefore, the system must be efficiently cooled in order to allow a fast and complete charging of the tank. In another study carried by Minko et al. [13], the authors perform the analysis of a model of a cylindrical metal hydride tank. They concluded that the concentration gradient in the bed was the main driving force of the hydrogen flow. Marty et al. [24] provided an experimental validation of numerical simulations of a metal hydride tank for a stationary co-generation system. Their goal was to achieve better performances against the compactness objectives.

Tsutomu et al. [25] provided a numerical model which was validated experimentally for a metal hydride vessel based on a plate-fin type heat exchanger. During the hydriding process, the model and the experimental results present a good agreement but during the dehydriding process, a big difference was observed concerning the calculated hydrogen desorption rates and the measured ones. This result was attributed to differences of heat transfer characteristics such as thermal conductivity of metal hydride particles and porosity between actual and assumed ones.

The absorption and desorption process are exothermic and endothermic reactions respectively, heat of reaction during absorption process may be stored and further used in desorption process. Therefore efficient ways are needed to supply the heat. Use of Phase Change Material (PCM) which can store latent heat is a recent and an attractive solution to resolve this issue. Mellouli et al. [26] presented a two-dimensional model describing the heat and mass transfer in metal hydride bed coupled to a PCM for storing heat. The model was made to compare two types of tank (cylindrical and spherical). The results showed that the latter exhibiting superior performance. The same model was investigated for  $laNi_5$  alloy by Rabienataj et al. [27] for charging and discharging processes. They found that inserting metal foam in the PCM jacket enhances the heat transfer by increasing the thermal conductivity, and significantly reduces the charging and discharging time. In another work, Mellouli et al. [28] developed a 3D mathematical model to investigate the influence of heat transfer fluid (HTF) and its mass flow rate on

hydrogen filling time for three various configurations of metal hydride tank (MH) (type 1: MH tank containing PCM heat exchanger, type 2: MH tank containing PCM heat exchanger and open HTF pipe and type 3: MH tank with PCM heat exchanger in which the HTF pipe was considered closed). They found that the type 2 was the most optimal regarding the hydrogen filling time and the HTF circulated with a higher mass flow rate has a favorable performance of the MH-PCM tank. BenMaad et al. [29] developed a two-dimensional (2D) mathematical model for a high temperature metal hydrogen reactor integrating a  $Mg_{69}Zn_{28}Al_3$  PCM. This solution was adopted to store efficiently the heat produced during hydrogen absorption process in order to reuse it during desorption. The obtained results showed that the new composition of PCM, which investigated by Garrier et al. [30] is the appropriate that met the requirements to store the heat released from the  $Mg_2Ni$  alloy and the time required for the reactor to desorb all the hydrogen do not exceed 2.5 h. The same PCM was used by Marty et al. [31] in order to study some modeling tools for the prediction of the time evolution of the various physical parameters such as front position, temperature, stored hydrogen volume, and fraction of the PCM which has been melted. A numerical study of the heat and mass transfers in an annular reactor has also been conducted in Ref. [32]. The results showed that the use of fins enhanced heat transfer and consequently lead to 40% improvement of the time required for the full charging of the hydride tank compared to the case without fins. Melnichuk et al. [33] focused on aluminum fraction optimization of heat exchanger fins for a  $LaNi_5$  hydride tank cylindrical, for different radius and at different absorption times. A two-dimensional axisymmetric model was developed by Ref. [34] to study the phenomena related to mass and heat transport inside a metal hydride canister. The model was validated experimentally. They concluded that the charging performances are strongly influenced by thermodynamic parameters: activation energy, thermal conductivity, absorption rate constant, and hydride porosity.

On thermal engineering, the application of Computational Fluid Dynamics (CFD) methods is frequently used to develop and design heat exchangers. R.Shaheen et al. [35] used this method to study numerically the hydrogen storage in metal hydride bed. They found that the amount of hydrogen adsorbed is greater than that of compressed hydrogen gas. A 3D modeling under Comsol Multiphysics of a cylindrical tank was carried out by Freni et al. [36]. Their study focused on the parameters to be optimized for a better hydrogen storage. Their results showed that the most relevant parameters were the hydrogen supply pressure, the permeability and the thermal conductivity of the hydride. The same observation was made with a 2D model developed by D.Chabane et al. [37] using Comsol Multiphysics. The same software was used by Bao et al. [38] to investigate a three-dimensional multiphysics model for metal hydride reactors, in which the velocity field of the heat transfer fluid was obtained by solving the Navier–Stokes equations. They studied effects of some parameters on the reactor performance. A three-dimensional(3D) hydrogen desorption model was developed by Kyoung et al. [39] to rigorously account for the principles of mass, momentum, energy conservation and hydrogen

desorption kinetics. The validity of their model was tested by a comparison with the experimental data reported by Jemni et al. [22]. Bhogilla et al. [40] developed a 3D numerical model for predicting the hydrogen absorption process performance of cylindrical metal hydride tank (MHT) filled with AB alloy type. A helical coil internal heat exchanger in the powdered metal hydride bed was used to control the heat exchanger between the MHT and the heat transfer fluid. The model was validated with the experimental data available in the literature. Elmas et al. [41] studied the effects of various parameters on the hydrogen absorption processes for three different metal alloys ( $MmNi_{4.6}Al_{0.4}$ ,  $LaNi_{4.75}Al_{0.25}$  and  $LaNi_5$ ). They concluded that the maximum amount of hydrogen mass to be stored was obtained by using  $LaNi_5$  but at the expense of the time charging. Keshari et al. [42] studied the transient behavior of sorption process inside the reactor using COMSOL Multiphysics 4.4. The model was compared to the experimental data obtained from the literature. Influence of various operating and geometric parameters on the total absorption time of the reactor has been investigated. The results showed that the most influencing factor to increase the absorption rate of hydrogen is the supply pressure.

Numerical study was carried out by Ref. [43] in order to optimise the geometrical parameters of both the hydride tank and exchanger using a COMSOL-MATLAB interface for three different designs. Brown et al. [44] developed a mathematical model describing the process of hydrogen storage in a commercial tank loaded with a metal hydride AB2 type. The obtained results allowed validating both the experimental measurements and the assumptions made for the modeling process. In the work by Artemov et al. [45], a numerical study concerning the hydrogen absorption process in rectangular metal hydride tanks have been done and validated experimentally for two types of reactors were - with and without aluminium foam. Results showed that the use of aluminium foam allows to perform a more effective system for hydrogen purification from impurities, compared to a case without aluminium foam.

More recent work on the hydride tank modeling is presented by Cui et al. [46]. They proposed a 3D model to study the heat behavior in thin double-layer annular ZrCo bed. The effects of conversion layer thickness, thermal conductivity, cooling medium and its flow velocity on the efficiency of the heat transfer were analysed by simulation.

All the models described in the literature review are typically developed and used to determine transport properties, reaction kinetics of metal-hydride systems, equilibrium conditions (pressure and temperature), and to study the technical aspects of the tank and cooling system designs. They are also used to investigate the effects of parameters on the thermodynamic behavior of the tank. Usually, Computational Fluid Dynamics (CFD) methods are used to solve these models. These methods require significantly more time and computing capacity to run. Anyway, there are several review articles which have addressed various aspects of hydride tank technologies, but to our knowledge none has specifically considered the energetic issues, which is the focus of this work. A 0D hydride tank model is well-suited for an energetic study and it allows fast simulation times (which is required for the future definition of energy management laws).

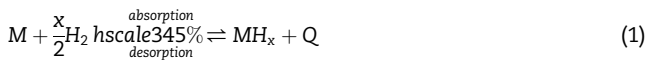
In this paper, the dynamic response of the hydrogen discharge from a hydride tank is studied to supply a 500 Watt fuel cell (PEMFC) generator. To this aim, a 0D simulation was performed with the MATLAB/Simulink software. After explaining the model principles and providing mathematical equations governing the heat and the mass transfer in the hydride tank, the model of the studied system is presented. Then, the experimental validation study of the hydride tank model is exposed. Finally, in order to demonstrate a possible dynamic interaction between the fuel cell generator and the hydride tank, especially in terms of heat and hydrogen pressure, key-results are presented and discussed.

## Mathematical modeling of the interaction between the hydride tank and the fuel cell

### Studied system

Many different kinds of models was proposed to describe and simulate the reaction kinetics, equilibrium conditions, heat and mass transfer inside the tank during absorption and desorption process [47–49]. A simplified sectional view of the hydride tank is shown in Fig. 1. The total length is 0.6[m], the outer diameter is 0.13[m], the inner diameter is 0.11[m]. 11.5[kg] of FeTi metal hydride alloy was contained in the tank. A tube type heat exchanger, made of copper, was installed in the tank with an outer diameter of 0.012[m].

The reversible interaction between the alloy with hydrogen gas can be expressed by the following equation [50]:



where  $M$  is the intermetallic matrix,  $H$  is hydrogen and  $Q$  is heat generating or providing by/to the metal hydride  $\text{MH}_x$  and  $x$  is the ratio of hydrogen to metal. The reaction is reversible and the direction is determined by the pressure (and temperature) of the hydrogen gas. If the pressure is above a certain level (the equilibrium pressure), the effect proceeds to the right to form hydride, whereas below the equilibrium pressure, hydrogen is liberated and the intermetallic matrix returns to its original state. The equilibrium pressure, itself, depends upon temperature.

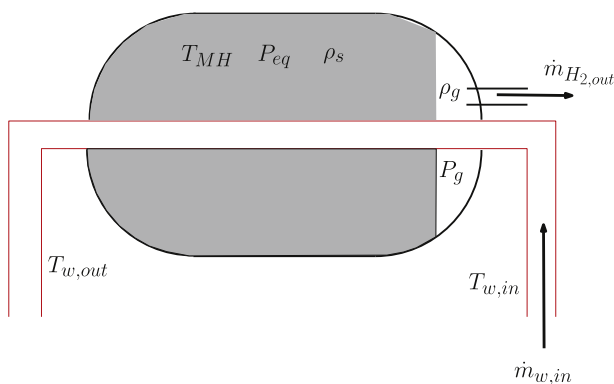


Fig. 1 – Synoptic of the model.

### Dynamic model of the hydride tank

In most cases, the first step of a mathematical modeling is to identify the appropriate assumptions to simplify the governing equations and enable them to be solved either analytically or numerically.

#### Assumptions of the model

The metal hydride bed is considered as a uniform mixture of a solid porous phase and a gaseous phase. This model incorporates the heat and mass balances that are applied to both metal hydride and hydrogen gas within the tank. The heat transfer from an external circulating water loop is taken into account.

Owing to the complexity of heat and mass transfer process, the following assumptions have been made to simplify the model formulations:

- the gas phase is ideal from the thermodynamic view point;
- there is a local thermal equilibrium between the gas and solid particles in the porous medium;
- the solid phase is isotropic;
- natural convection within the hydride powder is negligible;
- the radiative transfer in the porous medium is neglected;
- thermophysical properties are constant;
- the heat transfer coefficient assumed constant;
- mass flow rate of the water assumed constant.

The mathematical model describing the heat and mass transfer in porous media is based on the methods that are traditionally used in the continuous media of fluids mechanic. These methods consist of determining the local expression of conservation laws, namely: mass conservation, momentum conservation, and energy conservation.

Considering the previous assumptions, the behavior of the hydride in the tank is described as below.

#### Mass balance

According to the mass conservation law, the hydrogen ( $\text{H}_2$ ) concentration distribution in the metal hydride bed and its evolution as a function of time is expressed by:

$$\left( \frac{v_{\text{tank}}}{v_{\text{MH}}} - 1 + \varepsilon \right) \frac{\partial \rho_g}{\partial t} = -n_d - \frac{\dot{m}_{\text{H}_2, \text{out}}}{v_{\text{MH}}} \quad (2)$$

where  $n_d$  is the amount of desorbed hydrogen per unit volume and unit time which denotes the reaction rate for desorption,  $\rho_g$  is the gas density desorbed,  $\varepsilon$  denotes the porosity of the metal bed, which is assumed to be constant and uniform over the metal bed. The porosity  $\varepsilon = 0.5$  was assumed uniform over the metal bed. The porosity values reported in literature generally vary from 0.43 to 0.63 for FeTi[51–53].  $v_{\text{tank}}$  represents the volume of the tank and  $v_{\text{MH}}$  is the volume occupied by the alloy which is 70% of the tank volume. This ratio makes it possible to take into account the filling or not of the hydride tank. It represents a control volume. The straight term of the equation implies that the mass of hydrogen gas in the tank increases when hydrogen is desorbed from the hydride. This equation is reduced to its traditional form when the reservoir is filled with hydride.

$$\varepsilon \frac{\partial \rho_g}{\partial t} = -n_d - \frac{\dot{m}_{H_2out}}{V_{MH}} \quad (3)$$

$$v_{MH} = 0.7 v_{tank} \quad (4)$$

$\dot{m}_{H_2out}$  is the mass flow rate demanded by the PEMFC which can be calculated using the fuel cell modeling and through using the following equation by considering a hydrogen stoichiometry  $\lambda_{H_2}$  of 1. The latter is defined as the ratio between reactant feed (into the fuel cell) and reactant consumption (inside the fuel cell).

$$\dot{m}_{H_2out} = \lambda_{H_2} \frac{M_{H_2} N_{fc} I_{fc}}{2F} \quad (5)$$

$$= \lambda_{H_2} \frac{M_{H_2}}{2F} \frac{P_{fc}}{V_{fc}} \quad (6)$$

where  $\lambda_{H_2}$  is hydrogen stoichiometry,  $M_{H_2}$  denotes hydrogen molar mass,  $N_{fc}$  is the number of cell in the PEMFC,  $I_{fc}$  is the cell current (A),  $F$  is Faraday's constant,  $V_{fc}$  is the cell voltage (V) and  $P_{fc}$  is the electrical power that is expressed as:

$$P_{fc} = N_{fc} I_{fc} V_{fc} \quad (7)$$

Over time, the density of the metal powder ( $\rho_s$ ) changes due to hydrogen desorption. Therefore, a source term is added to the right-hand side in the mass balance equation of the solid (FeTi alloy) indicating the amount of hydrogen which is removed by the solid with time. The mass balance for the metal alloy (FeTi) is:

$$(1 - \varepsilon) \frac{\partial \rho_s}{\partial t} = n_d \quad (8)$$

#### Kinetics reaction

The amount of the hydrogen desorbed by the metal as a function of time is directly related to the reaction rate of the dehydriding (hydrogen desorption) process. The hydrogen desorption kinetic is strongly influenced by the thermodynamic conditions in the tank. It is expressed as follows:

$$n_d = C_d \exp\left(\frac{-E_d}{RT_{MH}}\right) \left(\frac{P_g - P_{eq}}{P_{eq}}\right) (\rho_s - \rho_0) \quad (9)$$

where  $C_d$  and  $E_d$  are the desorption rate constant and desorption activation energy respectively,  $R$  is the gas constant (8.314472 J/mol/K),  $\rho_0$  is the density of the metal hydride alloy when it has desorbed all of the hydrogen gas that can reversibly be desorbed.  $P_g$  is the pressure of the hydrogen gas and  $P_{eq}$  is the equilibrium pressure.

According to the ideal gas assumption, the hydrogen pressure in the tank is as follows:

$$P_g = \frac{\rho_g RT_{MH}}{M_{H_2}} \quad (10)$$

The equilibrium pressure can be described as a function of the temperature by vant Hoff equation [54–56]. Usually, it can be taken in the central of the equilibrium plateau of the PCT curve [12].

$$\ln\left(\frac{P_{eq}}{P_0}\right) = \frac{\Delta H}{RT} + \frac{-\Delta S}{R} \quad (11)$$

where  $P_0$  is atmospheric pressure,  $\Delta S$  and  $\Delta H$  are entropy and enthalpy changes of the dehydriding reaction, respectively,  $T$  is the absolute temperature. For any hydride solid, the change in entropy is approximately equivalent [1]. The thermodynamic parameters (enthalpy and entropy) of the hydride decomposition process can be obtained from the so-called vant Hoff plots that represent a variation with temperature of the equilibrium pressure logarithm derived from the PCT isotherms [12].

Another variant of this equation consists to express  $P_{eq}$  as a function of the hydride temperature and the Hydrogen-to-Metal atomic ratio (H/M), where  $H$  and  $M$  are, respectively, the number of hydrogen and metals atoms in the unit cell. It is calculated using experimental data as follows:

$$P_{eq} = f(H/M) \exp\left(-\frac{|\Delta H|}{R} \left(\frac{1}{T_{MH}} - \frac{1}{T_{ref}}\right)\right) \quad (12)$$

where:  $f(H/M)$  is the equilibrium pressure at the reference temperature  $T_{ref}$ . This function is given by fitting the experimental data of the PCT curve (Fig. 2) available in Ref. [12]. As shown in Fig. 2, the length of plateau translates the amount of  $H_2$  that can be stored reversibly with a small pressure variation.

The hydrogen desorbed is typically expressed as gravimetric storage capacity, wt%, referred to the mass of the desorbent ( $m_M$ ) and of the desorbed hydrogen,  $m_{H_2}$ , from a technological point of view, the capacity presentation in wt% is very useful, because it gives direct information on how much of hydrogen can be stored in a material.

$$wt\% = \frac{m_{H_2}}{m_M + m_{H_2}} 100 \quad (13)$$

Eq. (14) gives the mass of hydrogen desorbed from the metal hydride tank:

$$m_{H_2} = m_0 + v_{MH} \int n_d dt \quad (14)$$

With  $m_0$  is the initial mass of hydrogen which in our case is equal to 0.1278[kg].

The gravimetric storage capacity can also be calculated from the ratio of the mass of hydrogen stored within the metal or compound to the mass of the host material including the absorbed hydrogen [57].

$$wt\% = \frac{[H/M]M_{H_2}}{M_M + [H/M]M_{H_2}} 100 \quad (15)$$

where.

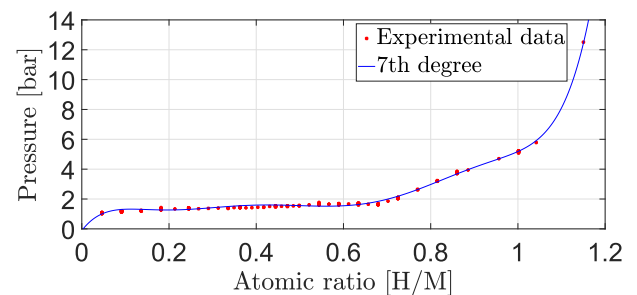


Fig. 2 – PCT curve of FeTi alloy at 21°C

- H/M: the hydrogen-to-metal ratio.
- $M_{H_2}$ : the molar mass of hydrogen.
- $M_M$ : the molar mass of metal.

Where, the hydrogen to metal ration is defined by Eq. (16) [58].

$$[H/M] = 2 \frac{(\rho_s - \rho_0)M_M}{\rho_0 M_{H_2}} \quad (16)$$

Finally, the equilibrium pressure for hydrogen desorption on FeTi is approximated as a 7th order polynomial function. Its coefficients are given in Table 1.

$$f(wt) = \sum_{i=0}^{n=7} a_i (wt\%)^i \quad (17)$$

### Energy equation

The desorption reaction is an endothermic process and it requires the following energy input to accomplish the desorption reaction:

$$\left( \epsilon \rho_g C_{p_g} + (1 - \epsilon) \rho_s C_{p_s} \right) \frac{\partial T_{MH}}{\partial t} = K_e \nabla^2 T_{MH} + Q + S_{TH} \quad (18)$$

where  $C_{p_g}$  and  $C_{p_s}$  are specific heat of the gas and solid phases respectively, the Laplacian temperature ( $\nabla^2 T_{MH}$ ) will be neglected by the assumption of a uniform distribution of temperature in the tank. Although the uniform temperature assumption does not accurately describe real phenomena, the difficulty of estimating the exact value of the heat transfer coefficient  $K_e$  is also present in multidimensional numerical modeling. The second term to the right of the equation above represents the amount of heat supplied by the heat transfer circuit to heat the hydride and bring it back to its equilibrium temperature. The third term reflects the internal heat source that is due to the endothermic reaction which is expressed as follows:

$$S_{TH} = n_d \frac{\Delta H_{des}}{M_{H_2}} \quad (19)$$

The total heat flux exchanged between the hydride and the heat transport circuit through the exchange surface element  $dS$ , as shown in Fig. 1, can be estimated by the following thermal balance model:

$$dQ = HdS(T - T_{HM}) = -\dot{m}_w C_{p_w} dT \quad (20)$$

where  $H, \dot{m}_w$  and  $C_{p_w}$  are the effective heat transfer coefficient [ $W/m^2$ ], mass flow rate of water [ $kg/s$ ], and the specific heat of the water [ $J/kg/K$ ] respectively.

By integrating (20) with the hypothesis of the uniformity of the temperature in the tank, the temperature at the exit of the heat transport circuit will be given by the following formula:

$$T_{w,out} = T_{MH} + (T_{w,in} - T_{MH}) e^{-\alpha} \quad (21)$$

where  $T_{w,in}$  is the inlet temperature of the circulation water channel which is set at 21°C. and:

$$\alpha = \frac{H \pi D L}{\dot{m}_w C_{p_w}} \quad (22)$$

where  $L$  and  $D$  are the length and the external diameter of the internal exchanger respectively.

The quantity of heat exchanged between the hydride and the heat transport circuit is obtained by per unit volume  $Q'$  transferred from the heat transport circuit to the tank and it can be expressed as follows:

$$Q' = \frac{\dot{m}_w C_{p_w}}{v_{MH}} (T_{w,in} - T_{MH}) (1 - e^{-\alpha}) \quad (23)$$

Then, the thermal power exchanged between the water circuit and the metal hydride is:

$$Q = Q' v_{HM} \quad (24)$$

### Initial conditions

The numerical model was used to simulate the same conditions experienced in the experimental work. Initial pressure for modeling is the same as that recorded by the pressure transducer during the experiments which is 15[bar]. For the initial tank temperature, it is adjusted equal to the heating fluid temperature 21°C. The hydride was assumed to be fully saturated with hydrogen, therefore, the initial density of metal alloy is considered equal to the saturated metal hydride density [59].

## Experimental validation of the hydride tank model

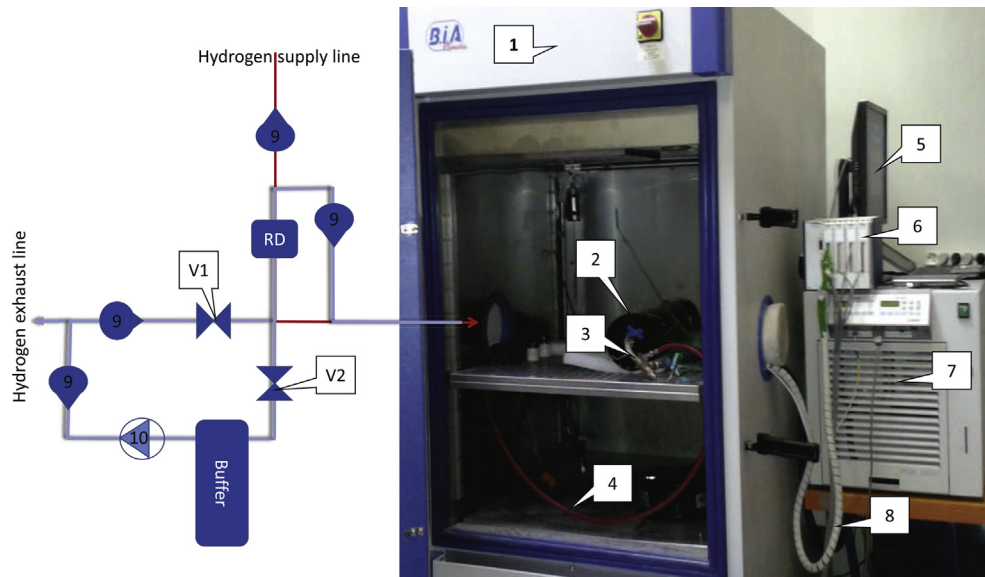
A test bench composed of ten main parts developed in the laboratory as shown in Fig. 3: (1) Climatic chamber, (2) Hydride tank, (3) Circuit of heat transport system, (4) Hydrogen line, (5) PC for system monitoring, (6) Acquisition card, (7) Hot/Cool generator, (8) thermocouple sensor (type K), (9) Check valve, (10) Vacuum pump, (V1 and 2) Valve and (RD) Flowmeter (Brooks 5850S). It allows the control and measurement of different operating parameters, such as a hydride temperature, temperature of the cooling water at input and output of the hydride tank, The hydrogen pressure, the mass flow rate.

### PCT process

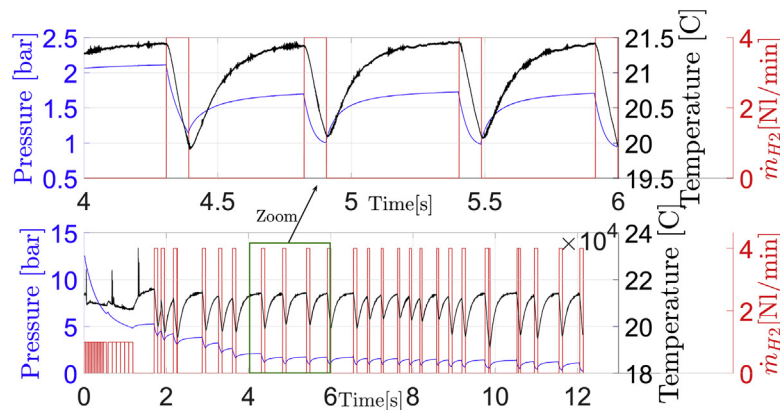
The tank is installed in a climatic chamber to control the ambient temperature (Fig. 3a). Initially, the tank is heated to a temperature of 21°C (gas valve closed). When the temperature in the tank is homogeneous, the gas exhaust valve is opened. The method consists in browsing the PCT pressure characteristics curve with a decrement factor of 5g (variation of the hydrogen mass amount). At first, at the start of the experiment, the hydrogen flow rate is fixed at 1 [Nl/min] (Fig. 3b). The temperature variations of the reservoir are then slow, of low amplitude and, consequently, of little significance in terms of measurement resolution for the energy characterization. Then a higher hydrogen flow of 4 [Nl/min] is selected. It corresponds to the rate at which a 500 Watt Proton Exchange

**Table 1 – Polynomial function of equilibrium pressure.**

	$a_0$	$a_1$	$a_2$	$a_3$
$10^3$	-0.001	0.0386	-0.388	1.8642
	$a_4$	$a_5$	$a_6$	$a_7$
$10^3$	-4.6387	6.14	-4.0849	1.0748



(a) Experimental test ben of hydride tank



(b) PCT experimental process

**Fig. 3 – Experimental set-up used for doing the PCT and energetic characterization of the hydride tank.**

Membrane Fuel Cell (PEMFC) will be fed. Heat is supplied to the tank through the heat transport circuit (water) which passes through the hydride bed of the tank with a constant flow rate of 1[l/min]. By imposing the amount of hydrogen desorbed, the system undergoes a decrease in temperature and pressure. Once the 5g threshold is reached, we stop the extraction of hydrogen, then we wait that the system return to equilibrium. The process is repeated until the complete extraction of the hydrogen from the tank.

The circuit supply/exhaust of hydrogen to/from the hydride tank is indicated in Fig. 3a at the left. During the absorption, the hydrogen is supplied to the tank through the first way (red line). During this phase, the valve V1 and V2 are closed. The second way (blue line) is used during the dehydriding process. For this characterization, two steps are considered depending on the hydrogen pressure at the outlet of the tank. If the hydrogen pressure is greater than the atmospheric pressure, the valve V1 is open and the valve V2 is closed. To characterize the hydride below the atmospheric pressure during the discharge, once the latter is reached (the

measurement is made by the differential pressure sensor), the hydrogen is channeled by the solenoid valve V2 to a buffer maintained in depression via a vacuum pump.

#### Energetic process

The test will consist in scanning the characteristic PCT curve in the direction of desorption by quantifying the energy exchanges involved. Heat exchanges are carried out using a hot/cold group (Fig. 3). The latter makes it possible to regulate the characterization temperature of the hydride. Two thermocouples are integrated into the heat transport circuit to measure the temperature variations at the tank inlet and outlet. The thermal power consumed by the hydride is expressed as follows:

$$Q = \dot{m}_w C p_w (T_{w_{in}} - T_{w_{out}}) \quad (25)$$

The control of the overall process is implemented on a National Instrument PCMCIA/SCXI platform using manual and/or automatic control software developed in the Labview

environment. The software interface allows the user to choose the running mode (absorption or desorption) and the parameters to be controlled. An interface panel allows the various available measurements, and sensor states to be checked. The measurements displayed and stored are the temperatures on the body of the tank, the ambient temperature, the pressure in the tank, the ambient pressure, the mass flow rate to calculate the amount of hydrogen absorbed or desorbed.

## Simulation of the hydride tank-fuel cell interaction

### Implementation of the simulation program

The aforementioned governing equations with the parameters from Table 1 are implemented under the MATLAB/Simulink software to simulate the dynamics of hydrogen discharge processes. The different blocks of Fig. 4 are related to the different governing equations (mass balance, kinetics reaction, and energy equation).

Hydrogen desorption is an endothermic process, which means that the hydrogen release process requires external energy input to accomplish the desorption reaction at a temperature equilibrium. In this study, the tank is heated by a water channel with a constant mass flow so that the temperature at the channel inlet is considered constant. The values of the parameters involved in the model (e.g. parameters related to the physical properties of the FeTi, with the modeling of the hydrogen line) are summarized in Table 2.

### Results and discussion

The experimental study focuses on the behavior of the hydride tank in order to validate the model included in Fig. 4. The fuel cell experimental will be considered in a future work.

In this work, some assumptions are made regarding fuel cell stack as:

- the hydrogen consumed is (according to the Faraday's law) directly proportional to the load current;
- the  $H_2$  is supplied to the tank with a stoichiometry rate of 1;
- the fuel cell temperature is constant;

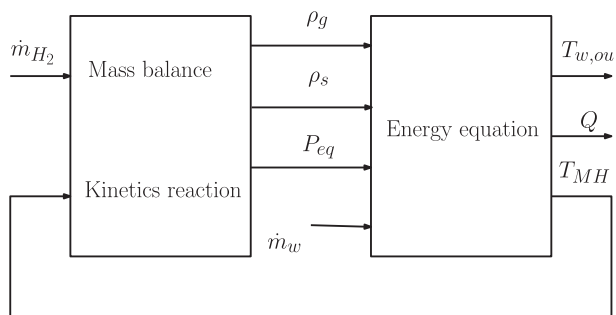


Fig. 4 – First layer of the Simulation diagram of hydrogen discharge processes implemented in MATLAB SIMULINK environment.

Table 2 – Parameters of the model.

$\epsilon$	0.5	
$v_c$	0.65	[m <sup>3</sup> ]
$C_d$	2.6 [59]	[1/s <sup>3</sup> ]
$E_d$	$19.87e^3$ [59]	[J/mol]
$M_{H_2}$	$2e^{-3}$	[kg/mol]
$M_M$	$103.7e^{-3}$	[kg/mol]
$m_M$	11.5	[kg]
$\rho_0$	6530	[kg/m <sup>3</sup> ]
$T_{ref}$	21	[°C]
$R$	8.314	[J/(mol*K)]
$Cp_g$	14890	[J/(kg*K)]
$Cp_s$	468	[J/(kg*K)]
$Cp_w$	4185	[J/(kg*K)]
$\Delta H$	$27.6e^3$ [59]	[J/mol]
$\dot{m}_w$	1	[l/min]
$T_{w,in}$	21	[°C]
$H$	600	[W/(m <sup>2</sup> *K)]
$D$	$1.2e^{-2}$	[m]
$D_{tank}$	$13e^{-2}$	[m]
$L$	$60e^{-2}$	[m]
$T_{fc}$	65	[°C]
$N_{fc}$	5	
$\lambda_{H_2}$	1	

- the number of cells in the stack is 5.

Fig. 5 depicts the  $H_2$  mass flow rate consumed by the 500 Watt fuel cell (PEMFC). This scenario is considered as the inlet of our model.

According to the hydrogen mass flow profile applied to the hydride tank, the total amount of the hydrogen desorbed from the hydride tank is 128 g as shown in Fig. 6a. This value is in agreement with the results found experimentally in our previous work [12]. As it can be seen, there is a gradual increase of the extracted hydrogen over time until the complete discharge of the tank, which is subordinated to the heat input. Fig. 6b represents the desorption kinetics of the hydrogen. This characteristic is an intrinsic characteristic of the metal hydride, but its evolution over time is strongly impacted by the consumption scenario of the fuel cell. As shown in Eq. (27), the heat produced by the fuel cell is related to its load current which is itself linked with the  $H_2$  mass flow rate consumed. In the same time, heat is used during the hydrogen desorption reaction, which is endothermic in nature. This heat has a direct impact on the kinetics reaction, therefore it's necessary to improve the heat transfer to achieve high dehydrogenation rate.

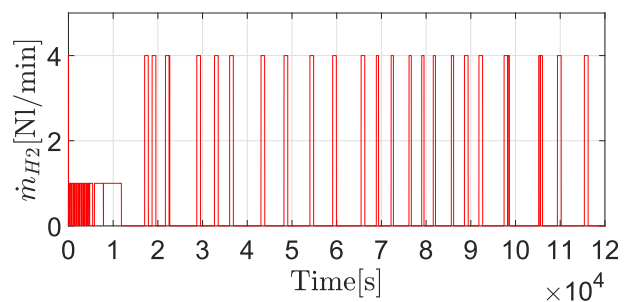
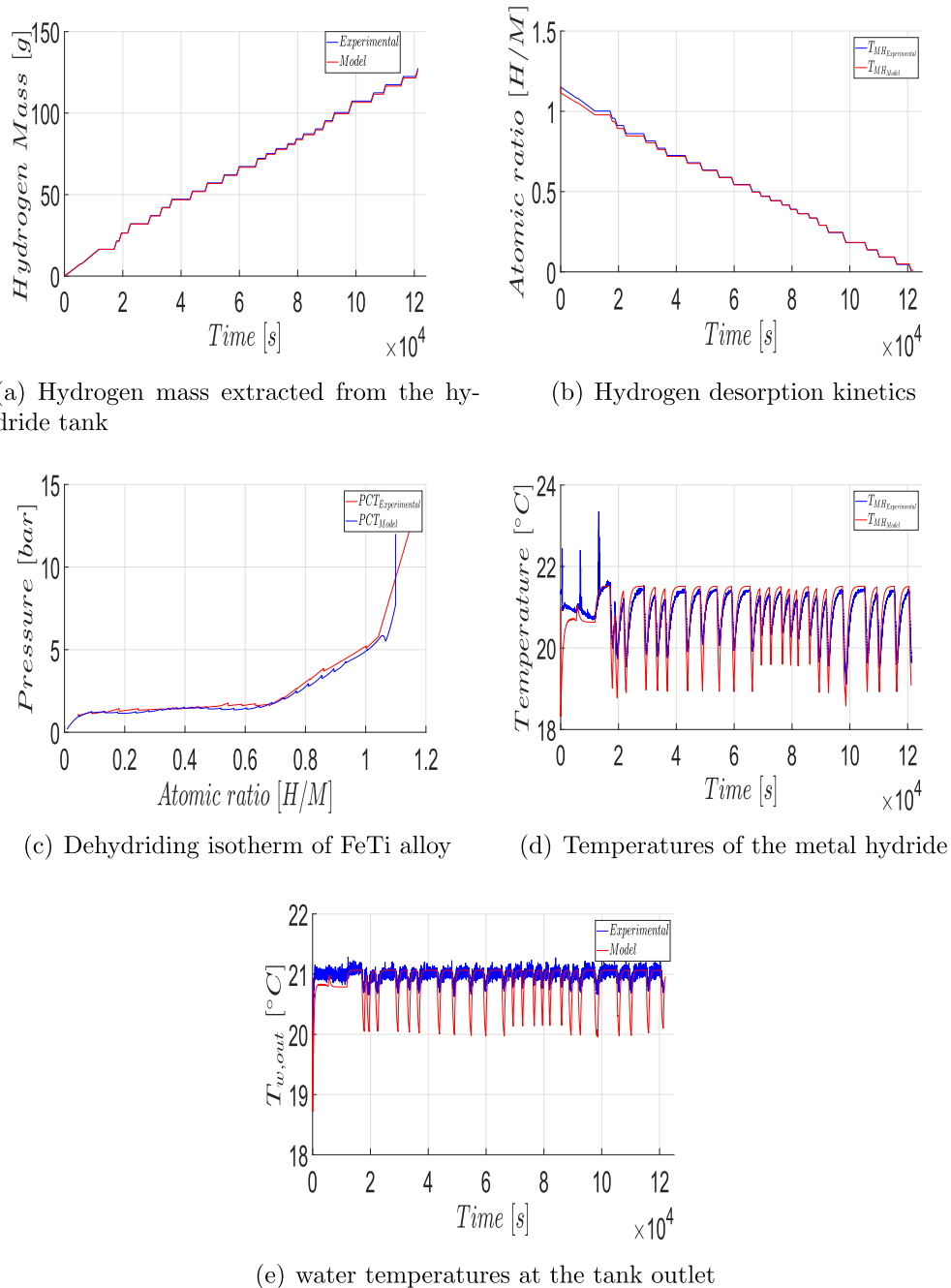


Fig. 5 – Profile of hydrogen mass flow.



**Fig. 6 – Experimental and simulation results.**

Fig. 6c shows the isotherm variation of the pressure concentration during the desorption process corresponding to the hydrogen mass flow extracted from the hydride tank. Since the unloading process is endothermic, the temperature in the hydride bed drops quickly (Fig. 6d). The drop observed at the beginning of the test (Fig. 6d) is caused by the evacuation of the hydrogen (through a valve opening) that was inside the tank in gaseous form. This opening of the valve induces a quick decreasing of the hydrogen pressure. Then, it continues to decrease up to reach the equilibrium pressure, which is 1.8 bar in our case as shown in Fig. 6c. At this value, the hydrogen desorption reaction will be started. The pressure oscillations result in changes in the temperature of the metal

hydride (Fig. 6d). These oscillations are induced by the dynamic variations of the hydrogen mass flow rate consumed by the fuel cell. In Fig. 6e, the temperature of the outlet of the heating water over time is shown. It can be seen that the heating temperature decreases to a value of 20°C throughout operation, also a downward spike can be seen for each cycle. This is caused by the sensible cooling that has to be done to heat the material to desorption temperature.

The accuracy of the proposed model was verified by measuring the Mean Absolute Percentage Error (MAPE) between the results of the proposed model and those obtained experimentally. It is defined by Eq. (26). The calculated MAPE value is 1.53% which indicates the good accuracy of the model.

However, we find that the model presents a dynamic more important than reality. There are surely some elements to refine because these strong temperature dynamics must result in strong power demand which may ultimately have an impact in the energy balance.

$$\text{MAPE} = \frac{100\%}{N} \sum_{i=1}^n \frac{|A_i - F_i|}{A_i} \quad (26)$$

where  $A_i$  and  $F_i$  denote the experimental and calculate values at data points respectively and  $N$  is the number of data points.

The heat generated by the fuel cell during the electro-chemical reaction can be calculated using the following equation:

$$Q_{fc} = I_{fc} N_{fc} (V_{oc} - V_{fc}) \quad (27)$$

where  $I_{fc}$  is the current of the fuel cell,  $N_{fc}$  is the number of cells in the stack,  $V_{oc}$  is the open circuit cell voltage and  $V_{fc}$  is the cell voltage.  $V_{oc}$  would be 1.48 V (if the water product is in liquid form) or 1.25 V (if the water product is in vapor form) [60].

The heat produced by the fuel cell and the heat consumed by the hydride in order to desorb the hydrogen is represented in Fig. 7. The simulation results show that the heat needed by the hydride to continue with the desorption process can be provided by the fuel cell. The maximum heat consumed by the hydride is about 70[W] and the heat that can be drawn from the fuel cell is about 300[W]. At the beginning of the desorption process, a rapid and significant amount of heat is consumed by the hydride. This system behavior is due to the quick fall of the tank pressure thus inducing a drop-down in the hydride temperature. In order to allow the continuity of the desorption process, a high consumption of calories by the hydride is required to break the bonds of the hydrogen with the metal.

Fig. 8 depicts the total energy used for hydrogen desorption wish is 3.7 [MJ]. This energy is representative of that measured experimentally. The theoretical energy for the same kind alloy is 1.7526 [MJ] according to [61,62]. There is a difference between these two values which can be explained as follows: the experimental value includes all measurement losses and errors on the different heat exchange circuits between the heat transfer unit, the hydride and the external environment, the error made in the determination of the limits of the two phases ( $\alpha$ ,  $\beta$ ), and a lack of knowledge of the exact composition of the hydride characterized (which has a direct impact on the concentration of hydrogen in the hydride).

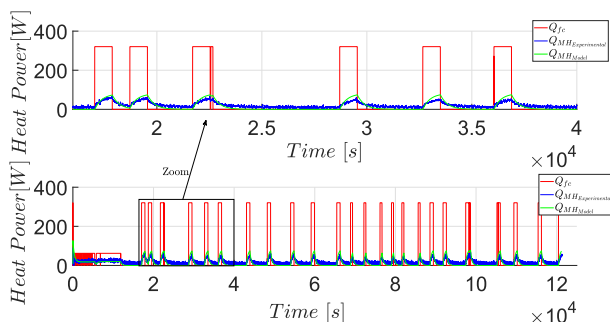


Fig. 7 – The heat produced by the fuel cell  $Q_{fc}$  and consumed by the metal hydride  $Q_{MH}$ .

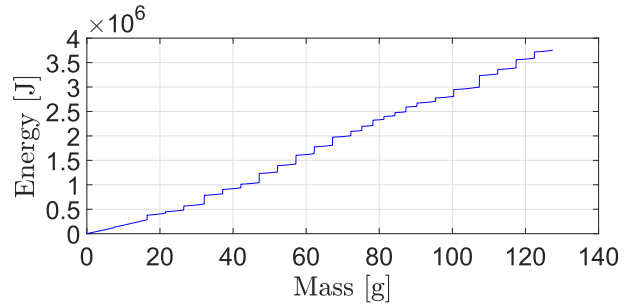


Fig. 8 – The energy consumed during the dihydriding process.

## Conclusion

The objective of the work was to develop an energetic model of tank that would be tractable in a simulation environment. A zero-dimensional model was developed for a MH tank for hydrogen storage, based on linked modular mathematical models in Matlab Simulink. The model was validated experimentally for a scenario of hydrogen consumption demand by a fuel cell system. Results are very close to those found experimentally, with maximum of 1.53% of error that is confirming the reliability of the mathematical model used to represent the performance of the metal hydride tank created in MATLAB. Also, the simulation results obtained with this model highlight the possibility of recovering the heat delivered by a PEMFC stack to extract the hydrogen from the hydride tank. Also, the simulations show and the strong dependence of the thermal behavior of the tank with the load profile imposed by the connected fuel cell generator.

Moreover, the results indicated a well-suited fluidic/thermal architecture as well as a good strategy of energy management need to be implemented in order to achieve an efficient thermal coupling between the fuel cell and the hydride tank. In future works, the proposed model can be used to achieve such an energetic control, and also examine the dynamics of fuel cell system performances incorporating enhanced control strategies of hydrogen supply with optimized control parameters.

This model can be also adapted for hydrogen absorption process, different alloys and experimental conditions.

## Acknowledgments

This research work is carried out thanks to two projects: MobyPost project funded under the Grant Agreement No.256834 by the European Union's seventh Framework program (FP7/2007e2013) for the Fuel Cell and Hydrogen Joint Technology Undertaking (<http://mobyproject.eu/>) and OenVHy project funded by the Bourgogne-Franche-Comté region-France.

## Nomenclature

Physics constants

$\Delta H$	heat of reaction [J/mol]
$\dot{m}$	mass flow rate [kg/s]
$\varepsilon$	porosity of metal hydride
$\lambda_{H_2}$	stoichiometry
$\rho$	density [Kg/m <sup>3</sup> ]
$C_d$	constant for hydrogen desorption rate [1/s]
$C_p$	specific heat [J/kg/K]
$D$	diameter [m]
$E_d$	activation energy [J/mol]
$F$	faraday constant
$H$	overall heat transfer coefficient [ $w/m^2K$ ]
$H/M$	hydrogen atoms per metal atom
$I$	current [A]
$i_{fc}$	current density [A/cm <sup>2</sup> ]
$K_e$	heat transfer coefficient [W/m/K]
$L$	length [m]
$m$	mass [kg]
$m_M$	masse of alloy [kg]
$M_{H_2}$	hydrogen molar mass [kg/mol]
$n_d$	hydrogen desorption kinetics [kg/sm <sup>3</sup> ]
$N_{fc}$	number of cells in the PEMFC stack
$P$	pressure [bar]
$Q$	heat flow [watt]
$R$	universal gas constant [J/mol/K]
$S_{TH}$	Internal heat source [J/m <sup>3</sup> s]
$T$	temperature [K]
$t$	time [s]
$V$	voltage [V]
$v$	volume [m <sup>3</sup> ]

## Subscripts

$O$	empty
$eq$	equilibrium
$fc$	fuel cell
$g$	
$in$	inlet
$M$	metal
$MH$	metal hydride
$oc$	open circuit
$out$	outlet
$ref$	reference
$s$	solid
$w$	water

## REFERENCES

- [1] Chaise A. Etude expérimentale et numérique de réservoirs d'hydrure de magnésium. Ph.D. thesis, Université Joseph-Fourier-Grenoble I. 2008. <https://tel.archives-ouvertes.fr/tel-00351465/>.
- [2] Zhu D, Chabane D, Ait-Amirat Y, N'Diaye A, Djerdir A. Estimation of the state of charge of a hydride hydrogen tank for vehicle applications. In: 2017 IEEE vehicle power and propulsion conference (VPPC). IEEE; 2017. p. 1–6. <https://doi.org/10.1109/VPPC.2017.8330976>. <http://ieeexplore.ieee.org/document/8330976>.
- [3] Amory B. LOVINS, twenty hydrogen myths. 2005. [www.rmi.org](http://www.rmi.org).
- [4] Sandi Giselle. Hydrogen storage and its limitations. The Electrochemical Society interface 2004;13:40–5. <https://www.electrochem.org/dl/interface/fal/fal04/IF8-04-Pages40-44.pdf>.
- [5] Züttel A. Hydrogen storage methods. *Naturwissenschaften* 2004;91:157–72. <https://doi.org/10.1007/s00114-004-0516-x>. [http://lem.ch.unito.it/didattica/infocimica/Idrogeno{\\\_}\\\_}2005/documenti/Review{\\\_}\\\_}Zuettel{\\\_}\\\_}2004.pdf](http://lem.ch.unito.it/didattica/infocimica/Idrogeno{\_}\_}2005/documenti/Review{\_}\_}Zuettel{\_}\_}2004.pdf).
- [6] Corgnale C, Hardy BJ, Anton DL. Structural analysis of metal hydride-based hybrid hydrogen storage systems. *Int J Hydrogen Energy* 2012;37(19):14223–33. <https://doi.org/10.1016/j.ijhydene.2012.06.040>. <http://linkinghub.elsevier.com/retrieve/pii/S0360319912013870>.
- [7] Patil SD, Ram Gopal M. Analysis of a metal hydride reactor for hydrogen storage. *Int J Hydrogen Energy* 2013;38(2):942–51. <https://doi.org/10.1016/j.ijhydene.2012.10.031>. <http://linkinghub.elsevier.com/retrieve/pii/S0360319912023191>.
- [8] Dinachandran L, Mohan G. Numerical simulation of the parametric influence on the wall strain distribution of vertically placed metal hydride based hydrogen storage container. *Int J Hydrogen Energy* 2015;40(16):5689–700. <https://doi.org/10.1016/j.ijhydene.2015.02.067>. <http://linkinghub.elsevier.com/retrieve/pii/S036031991500422X>.
- [9] Lototskyy MV, Davids MW, Tolj I, Klochko YV, Sekhar BS, Chidziva S, et al. Metal hydride systems for hydrogen storage and supply for stationary and automotive low temperature PEM fuel cell power modules. *Int J Hydrogen Energy* 2015;40(35):11491–7. <https://doi.org/10.1016/j.ijhydene.2015.01.095>. <http://linkinghub.elsevier.com/retrieve/pii/S0360319915001639>.
- [10] Mellouli S, Abhilash E, Askri F, Ben Nasrallah S. Integration of thermal energy storage unit in a metal hydride hydrogen storage tank. *Appl Therm Eng* 2016;102:1185–96. <https://doi.org/10.1016/j.applthermaleng.2016.03.116>. <http://linkinghub.elsevier.com/retrieve/pii/S1359431116304203>.
- [11] Chibani A, Bougriou C. Effect of the tank geometry on the storage and destocking of hydrogen on metal hydride (LaNi<sub>5</sub>H<sub>2</sub>). *Int J Hydrogen Energy* 2017;42(36):23035–44. <https://doi.org/10.1016/j.ijhydene.2017.07.102>. <http://linkinghub.elsevier.com/retrieve/pii/S0360319917329282>.
- [12] Chabane D, Harel F, Djerdir A, Candusso D, ElKedim O, Fenineche N. A new method for the characterization of hydrides hydrogen tanks dedicated to automotive applications. *Int J Hydrogen Energy* 2016;41(27):11682–91. <https://doi.org/10.1016/j.ijhydene.2015.12.048>. <http://www.sciencedirect.com/science/article/pii/S0360319915304146>.
- [13] Minko K, Artemov V, Yan'kov G. Numerical simulation of sorption/desorption processes in metal-hydride systems for hydrogen storage and purification. Part II: verification of the mathematical model. *Int J Heat Mass Tran* 2014;68:693–702. <https://doi.org/10.1016/j.ijheatmasstransfer.2013.09.057>. <http://www.sciencedirect.com/science/article/pii/S0017931013008314>.
- [14] Boukhari A, Bessaïh R. Numerical heat and mass transfer investigation of hydrogen absorption in an annulus-disc reactor. *Int J Hydrogen Energy* 2015;40(39):13708–17. <https://doi.org/10.1016/j.ijhydene.2015.05.123>. <http://www.sciencedirect.com/science/article/pii/S0360319915013270>.
- [15] Maeda T, Nishida K, Tange M, Takahashi T, Nakano A, Ito H, et al. Numerical simulation of the hydrogen storage with reaction heat recovery using metal hydride in the totalized hydrogen energy utilization system. *Int J Hydrogen Energy* 2011;36(17):10845–54. <https://doi.org/10.1016/j.ijhydene.2011.06.024>. <http://www.sciencedirect.com/science/article/pii/S0360319911014649>.
- [16] G. Momen, Modélisation numérique et étude expérimentale du stockage de l'hydrogène dans des réservoirs à lit fixe adsorbants, <http://www.theses.fr>. Available from: <http://www.theses.fr/2006PA132026>.

- [17] J. Nam, J. Ko, H. Ju, Three-dimensional modeling and simulation of hydrogen absorption in metal hydride hydrogen storage vessels, *Applied energy*. Available from: <http://www.sciencedirect.com/science/article/pii/S0306261911004004>.
- [18] P. Muthukumar, U. Madhavakrishna, A. Dewan, Parametric studies on a metal hydride based hydrogen storage device, *Int J*. Available from: <http://www.sciencedirect.com/science/article/pii/S0360319907004715>.
- [19] El Osery I. Theory of the computer code RET 1 for the calculation of space-time dependent temperature and composition properties of metal hydride hydrogen storage beds. *Int J Hydrogen Energy* 1983;8(3):191–8. [https://doi.org/10.1016/0360-3199\(83\)90064-2](https://doi.org/10.1016/0360-3199(83)90064-2). <https://www.sciencedirect.com/science/article/pii/0360319983900642>.
- [20] Lucas G, Richards W. Mathematical modelling of hydrogen storage systems. *Int J Hydrogen Energy* 1984;9(3):225–31. [https://doi.org/10.1016/0360-3199\(84\)90123-X](https://doi.org/10.1016/0360-3199(84)90123-X). <https://www.sciencedirect.com/science/article/pii/036031998490123X>.
- [21] Mayer U, Groll M, Supper W. Heat and mass transfer in metal hydride reaction beds: experimental and theoretical results. *J Less Common Met* 1987;131(1–2):235–44. [https://doi.org/10.1016/0022-5088\(87\)90523-6](https://doi.org/10.1016/0022-5088(87)90523-6). <https://www.sciencedirect.com/science/article/pii/0022508887905236>.
- [22] Jemni A. Study of two-dimensional heat and mass transfer during absorption in a metal-hydrogen reactor. *Int J Hydrogen Energy* 1995;20(1):43–52. [https://doi.org/10.1016/0360-3199\(93\)E0007-8](https://doi.org/10.1016/0360-3199(93)E0007-8). <http://linkinghub.elsevier.com/retrieve/pii/S0360319993E00078>.
- [23] Dogan A, Kaplan Y, Veziroglu T. Numerical investigation of heat and mass transfer in a metal hydride bed. *Appl Math Comput* 2004;150(1):169–80. [https://doi.org/10.1016/S0096-3003\(03\)00207-8](https://doi.org/10.1016/S0096-3003(03)00207-8). <http://www.sciencedirect.com/science/article/pii/S0096300303002078>.
- [24] Marty P, Fourmigue J-F, Rango PD, Fruchart D, Charbonnier J. Numerical simulation of heat and mass transfer during the absorption of hydrogen in a magnesium hydride. *Energy Convers Manag* 2006;47(20):3632–43. <https://doi.org/10.1016/j.enconman.2006.03.014>. <http://www.sciencedirect.com/science/article/pii/S0196890406000732>.
- [25] Oi T, Maki K, Sakaki Y. Heat transfer characteristics of the metal hydride vessel based on the plate-fin type heat exchanger. *J Power Sources* 2004;125(1):52–61. [https://doi.org/10.1016/S0378-7753\(03\)00822-X](https://doi.org/10.1016/S0378-7753(03)00822-X). <https://www.sciencedirect.com/ezproxy.utbm.fr/science/article/pii/S037877530300822X>.
- [26] Mellouli S, Ben Khedher N, Askri F, Jemni A, Ben Nasrallah S. Numerical analysis of metal hydride tank with phase change material. *Appl Therm Eng* 2015;90:674–82. <https://doi.org/10.1016/J.APPLTHERMALENG.2015.07.022>. <https://www.sciencedirect.com/ezproxy.utbm.fr/science/article/pii/S1359431115006870>.
- [27] Rabienataj Darzi AA, Hassanzadeh Afrouzi H, Moshfegh A, Farhadi M. Absorption and desorption of hydrogen in long metal hydride tank equipped with phase change material jacket. *Int J Hydrogen Energy* 2016;41(22):9595–610. <https://doi.org/10.1016/J.IJHYDENE.2016.04.051>. <https://www.sciencedirect.com/ezproxy.utbm.fr/science/article/pii/S0360319916301586>.
- [28] Mellouli S, Askri F, Abhilash E, Ben Nasrallah S. Impact of using a heat transfer fluid pipe in a metal hydride-phase change material tank. *Appl Therm Eng* 2017;113:554–65. <https://doi.org/10.1016/J.APPLTHERMALENG.2016.11.065>. <https://www.sciencedirect.com/ezproxy.utbm.fr/science/article/pii/S1359431116331544>.
- [29] Ben Mâad H, Askri F, Virgone J, Ben Nasrallah S. Numerical study of high temperature metal-hydrogen reactor (Mg<sub>2</sub>Ni-H<sub>2</sub>) with heat reaction recovery using phase-change material during desorption. *Appl Therm Eng* 2018;140:225–34. <https://doi.org/10.1016/J.APPLTHERMALENG.2018.05.009>. <https://www.sciencedirect.com/science/article/pii/S1359431118307142>.
- [30] Garrier S, Delhomme B, de Rango P, Marty P, Fruchart D, Miraglia S. A new MgH<sub>2</sub> tank concept using a phase-change material to store the heat of reaction. *Int J Hydrogen Energy* 2013;38(23):9766–71. <https://doi.org/10.1016/J.IJHYDENE.2013.05.026>. <https://www.sciencedirect.com/science/article/pii/S0360319913011889>.
- [31] Marty P, de Rango P, Delhomme B, Garrier S. Various tools for optimizing large scale magnesium hydride storage. *J Alloy Comp* 2013;580:S324–8. <https://doi.org/10.1016/J.JALLCOM.2013.02.169>. <https://www.sciencedirect.com/science/article/pii/S0925838813005100>.
- [32] Askri F, Ben Salah M, Jemni A, Ben Nasrallah S. Heat and mass transfer studies on metal-hydrogen reactor filled with MmNi<sub>4</sub>Fe<sub>0.4</sub>. *Int J Hydrogen Energy* 2009;34(16):6705–11. <https://doi.org/10.1016/j.ijhydene.2009.06.069>. <http://www.sciencedirect.com/science/article/pii/S0360319909009707>.
- [33] Melnichuk M, Silin N, Peretti H. Optimized heat transfer fin design for a metal-hydride hydrogen storage container. *Int J Hydrogen Energy* 2009;34(8):3417–24. <https://doi.org/10.1016/J.IJHYDENE.2009.02.040>. <https://www.sciencedirect.com/science/article/pii/S0360319909002250>.
- [34] Busqué R, Torres R, Grau J, Roda V, Husar A. Effect of metal hydride properties in hydrogen absorption through 2D-axisymmetric modeling and experimental testing in storage canisters. *Int J Hydrogen Energy* 2017;42(30):19114–25. <https://doi.org/10.1016/J.IJHYDENE.2017.06.125>. <https://www.sciencedirect.com/ezproxy.utbm.fr/science/article/pii/S0360319917324448>.
- [35] Ye F, Xiao J, Hu B, Benard P, Chahine R. Implementation for model of adsorptive hydrogen storage using UDF in fluent. *Physics Procedia* 2012;24:793–800. <https://doi.org/10.1016/j.phpro.2012.02.118>. <http://linkinghub.elsevier.com/retrieve/pii/S1875389212001617>.
- [36] Freni A, Cipit F, Cacciola G. Finite element-based simulation of a metal hydride-based hydrogen storage tank. *Int J Hydrogen Energy* 2009;34:8574–82. <https://doi.org/10.1016/j.ijhydene.2009.07.118>. [https://ac-els-cdn-com.ezproxy.utbm.fr/S0360319909012026/1-s2.0-S0360319909012026-main.pdf?{\\\_}tid=069f6b50-9e7b-4d4c-9511-148dc53e6b5f{\\\_}&jacdnat=1534913259{\\\_}54b2da251b3581a7069162a46a031fc0](https://ac-els-cdn-com.ezproxy.utbm.fr/S0360319909012026/1-s2.0-S0360319909012026-main.pdf?{\_}tid=069f6b50-9e7b-4d4c-9511-148dc53e6b5f{\_}&jacdnat=1534913259{\_}54b2da251b3581a7069162a46a031fc0).
- [37] Chabane D, Harel F, Djerdir A, Ibrahim M, Candusso D, Elkedim O, et al. Influence of the key parameters on the dynamic behavior of the hydrogen absorption by LaNi<sub>5</sub>. *Int J Hydrogen Energy* 2017;42(2):1412–9. <https://doi.org/10.1016/j.ijhydene.2016.06.110>. <http://linkinghub.elsevier.com/retrieve/pii/S0360319916306449>.
- [38] Bao Z, Wu Z, Nyamsi SN, Yang F, Zhang Z. Three-dimensional modeling and sensitivity analysis of multi-tubular metal hydride reactors. *Appl Therm Eng* 2013;52(1):97–108. <https://doi.org/10.1016/J.APPLTHERMALENG.2012.11.023>. <https://www.sciencedirect.com/ezproxy.utbm.fr/science/article/pii/S1359431112007363>.
- [39] Kyoung S, Ferekh S, Gwak G, Jo A, Ju H. Three-dimensional modeling and simulation of hydrogen desorption in metal hydride hydrogen storage vessels. *Int J Hydrogen Energy* 2015;40(41):14322–30. <https://doi.org/10.1016/J.IJHYDENE.2015.03.114>. <https://www.sciencedirect.com/ezproxy.utbm.fr/science/article/pii/S0360319915007582>.
- [40] Bhogilla SS. Design of a AB<sub>2</sub>-metal hydride cylindrical tank for renewable energy storage. *J Energy Storage* 2017;14:203–10. <https://doi.org/10.1016/J.EST.2017.10.012>.

- <https://www-sciencedirect-com.ezproxy.utbm.fr/science/article/pii/S2352152X1730289X>.
- [41] Elmas U, Bedir F, Kayfeci M. Computational analysis of hydrogen storage capacity using process parameters for three different metal hydride materials. *Int J Hydrogen Energy* 2018;43(23):10741–54. <https://doi.org/10.1016/J.IJHYDENE.2017.12.057>. <https://www-sciencedirect-com.ezproxy.utbm.fr/science/article/pii/S0360319917346955>.
- [42] Keshari V, Maiya M. Design and investigation of hydriding alloy based hydrogen storage reactor integrated with a pin fin tube heat exchanger. *Int J Hydrogen Energy* 2018;43(14):7081–95. <https://doi.org/10.1016/J.IJHYDENE.2018.02.100>. <https://www-sciencedirect-com.ezproxy.utbm.fr/science/article/pii/S0360319918305676{\#}!>.
- [43] Raju M, Kumar S. System simulation modeling and heat transfer in sodium alanate based hydrogen storage systems. *Int J Hydrogen Energy* 2011;36(2):1578–91. <https://doi.org/10.1016/J.IJHYDENE.2010.10.100>. <https://www-sciencedirect-com/science/article/pii/S0360319910022202>.
- [44] Brown TM, Brouwer J, Samuelsen GS, Holcomb FH, King J. Accurate simplified dynamic model of a metal hydride tank. *Int J Hydrogen Energy* 2008;33(20):5596–605. <https://doi.org/10.1016/j.ijhydene.2008.05.104>. <http://linkinghub.elsevier.com/retrieve/pii/S0360319908006538>.
- [45] Artemov VI, Minko KB, Yan'kov GG. Numerical study of heat and mass transfer processes in a metal hydride reactor for hydrogen purification. *Int J Hydrogen Energy* 2016;41(23):9762–8. <https://doi.org/10.1016/J.IJHYDENE.2016.01.124>. <https://www-sciencedirect-com.ezproxy.utbm.fr/science/article/pii/S0360319916001695>.
- [46] Y. Cui, X. Zeng, H. Kou, J. Ding, F. Wang, Numerical modeling of heat transfer during hydrogen absorption in thin double-layered annular ZrCo beds, *Results in Physics*. doi:10.1016/j.rinp.2018.03.011. Available from: <http://linkinghub.elsevier.com/retrieve/pii/S221137971732421X>.
- [47] Sakintuna B, Lamari-Darkrim F, Hirscher M. Metal hydride materials for solid hydrogen storage: a review. *Int J Hydrogen Energy* 2007;32(9):1121–40. <https://doi.org/10.1016/J.IJHYDENE.2006.11.022>. <https://www-sciencedirect-com/science/article/pii/S0360319906005866>.
- [48] Ren J, Musyoka NM, Langmi HW, Mathe M, Liao S. Current research trends and perspectives on materials-based hydrogen storage solutions: a critical review. *Int J Hydrogen Energy* 2017;42(1):289–311. <https://doi.org/10.1016/J.IJHYDENE.2016.11.195>. <https://www-sciencedirect-com/science/article/pii/S0360319916335285>.
- [49] Liu J, Zheng Z, Cheng H, Li K, Yan K, Han X, et al. Long-term hydrogen storage performance and structural evolution of LaNi<sub>4</sub>Al alloy. *J Alloy Comp* 2018;731:172–80. <https://doi.org/10.1016/J.JALLCOM.2017.10.042>. <https://www-sciencedirect-com/science/article/pii/S0925838817334564>.
- [50] Afzal M, Mane R, Sharma P. Heat transfer techniques in metal hydride hydrogen storage: a review. *Int J Hydrogen Energy* 2017;42(52):30661–82. <https://doi.org/10.1016/J.IJHYDENE.2017.10.166>. <https://www-sciencedirect-com/science/article/pii/S0360319917342726{\#}bib5>.
- [51] Jemni A, Nasrallah SB, Lamloumi J. Experimental and theoretical study of a metal hydrogen reactor. *Int J Hydrogen Energy* 1999;24(7):631–44. [https://doi.org/10.1016/S0360-3199\(98\)00117-7](https://doi.org/10.1016/S0360-3199(98)00117-7). <https://www-sciencedirect-com/science/article/pii/S0360319998001177?via{\%}I3Dihub>.
- [52] Askri F, Jemni A, Ben Nasrallah S. Prediction of transient heat and mass transfer in a closed metalhydrogen reactor. *Int J Hydrogen Energy* 2004;29(2):195–208. [https://doi.org/10.1016/S0360-3199\(03\)00089-2](https://doi.org/10.1016/S0360-3199(03)00089-2). <https://www-sciencedirect-com/science/article/pii/S0360319903000892>.
- [53] Askri F, Jemni A, Ben Nasrallah S. Dynamic behavior of metalhydrogen reactor during hydriding process. *Int J Hydrogen Energy* 2004;29(6):635–47. [https://doi.org/10.1016/S0360-3199\(03\)00220-9](https://doi.org/10.1016/S0360-3199(03)00220-9). <https://www-sciencedirect-com/science/article/pii/S0360319903002209>.
- [54] Hardy BJ, Anton DL. Hierarchical methodology for modeling hydrogen storage systems. Part II: detailed models. *Int J Hydrogen Energy* 2009;34(7):2992–3004. <https://doi.org/10.1016/J.IJHYDENE.2008.12.056>. <https://www-sciencedirect-com/science/article/pii/S0360319908017655>.
- [55] Hardy BJ, Anton DL. Hierarchical methodology for modeling hydrogen storage systems. Part I: scoping models. *Int J Hydrogen Energy* 2009;34(5):2269–77. <https://doi.org/10.1016/J.IJHYDENE.2008.12.070>. <https://www-sciencedirect-com/science/article/pii/S0360319908017722>.
- [56] Nyamsi SN, Yang F, Zhang Z. An optimization study on the finned tube heat exchanger used in hydride hydrogen storage system analytical method and numerical simulation. *Int J Hydrogen Energy* 2012;37(21):16078–92. <https://doi.org/10.1016/J.IJHYDENE.2012.08.074>. <https://www-sciencedirect-com/science/article/pii/S0360319912018769>.
- [57] Sandrock G. A panoramic overview of hydrogen storage alloys from a gas reaction point of view. *J Alloy Comp* 1999;293–295:877–88. [https://doi.org/10.1016/S0925-8388\(99\)00384-9](https://doi.org/10.1016/S0925-8388(99)00384-9). <https://www-sciencedirect-com/science/article/pii/S0925838899003849>.
- [58] R. Busqué, R. Torres, J. Grau, V. Roda, A. Husar, Mathematical modeling, numerical simulation and experimental comparison of the desorption process in a metal hydride hydrogen storage system, *Int J Hydrogen Energy*. doi:10.1016/J.IJHYDENE.2017.12.172. Available from: <https://www-sciencedirect-com/science/article/pii/S0360319917348930>.
- [59] Zeaiter A, Chapelle D, Perreux D, Thiebaud F, Nardin P. Macro-modeling of a hydrogen solid storage cylindrical tank. *Energy Procedia* 2015;74:1440–51. <https://doi.org/10.1016/J.EGYPRO.2015.07.791>. <https://www-sciencedirect-com/science/article/pii/S1876610215015593>.
- [60] Tetuko AP, Shabani B, Andrews J. Thermal coupling of PEM fuel cell and metal hydride hydrogen storage using heat pipes. *Int J Hydrogen Energy* 2016;41(7):4264–77. <https://doi.org/10.1016/J.IJHYDENE.2015.12.194>. <https://www-sciencedirect-com/science/article/pii/S0360319915313501>.
- [61] SARKAR A, BANERJEE R. Net energy analysis of hydrogen storage options. *Int J Hydrogen Energy* 2005;30(8):867–77. <https://doi.org/10.1016/j.ijhydene.2004.10.021>. <http://linkinghub.elsevier.com/retrieve/pii/S0360319904003738>.
- [62] Cohen RL, Wernick JH. Hydrogen storage materials: properties and possibilities. *Science* 1981;214(4525):1081–7. <https://doi.org/10.1126/science.214.4525.1081>. <http://www-sciencemag.org/cgi/doi/10.1126/science.214.4525.1081>.